

Chiral skyrmions in thin magnetic films: new objects for magnetic storage technologies?

N. S. Kiselev, A. N. Bogdanov, R. Schäfer, and U. K. Röbner*
IFW Dresden, Postfach 270116, D-01171 Dresden, Germany

Axisymmetric magnetic lines of nanometer sizes (chiral *vortices* or *skyrmions*) have been predicted to exist in a large group of noncentrosymmetric crystals more than two decades ago. Recently these magnetic textures have been directly observed in nanolayers of cubic helimagnets and monolayers of magnetic metals. We develop a micromagnetic theory of chiral skyrmions in thin magnetic layers for magnetic materials with intrinsic and induced chirality. Such particle-like and stable micromagnetic objects can exist in broad ranges of applied magnetic fields including zero field. Chiral skyrmions can be used as a new type of highly mobile nanoscale data carriers.

PACS numbers: 75.70.Cn, 75.50.Ee, 75.30.Kz, 85.70.Li,

In magnetic materials with broken chiral symmetry the structural handedness induces chiral Dzyaloshinskii-Moriya (DM) couplings [1] which stabilize two- and three-dimensional localized structures with a fixed rotation sense and nanometer sizes [2, 3]. Originally, they have been described as chiral vortex-like configurations, but they are smooth and stable, topologically non-trivial magnetization configurations and, therefore, can be identified as *skyrmions* in the micromagnetic limit with constant magnetization modulus, $|\mathbf{M}| = \text{const}$. These skyrmions differ from other axisymmetric patterns induced by external dipole-dipole forces (bubble domains in nanolayers [4] and magnetic vortices in magnetic nanodots [5]). Importantly, chiral skyrmions can also arise in nanolayers of magnetic metals where they are stabilized by surface/interface induced DM interactions [6]. In common (centrosymmetric) magnetic crystals such solitonic states are radially unstable and collapse spontaneously under the influence of the applied field or anisotropy [2]. This singles out magnets with intrinsic and induced DM interactions into a particular class of magnetic materials where nanoscale magnetic solitons exist [3].

Recently, observations of such chiral skyrmions have been reported in nanolayers of noncentrosymmetric cubic ferromagnets (Fe,Co)Si and FeGe [7] and in monolayers of Fe with a strong surface induced DM coupling [8]. This experimental break-through is not only an impressive demonstration of a unique phenomenon: static solitons and formation of solitonic mesophases in a chiral condensed matter system [3]. These experiments also constitute new avenue for magnetic data storage and spintronics technologies. Chiral skyrmions, as magnetic inhomogeneities localized into spots of a few nanometer, can be freely created and manipulated, e.g., in extended layers of *magnetically soft materials*. These countable objects allow to fulfill a key task in creating versatile magnetic patterns at the nanoscale.

This letter formulates the basic micromagnetic theory for thin ferromagnetic layers with chiral DM couplings and presents equilibrium solutions of isolated skyrmions

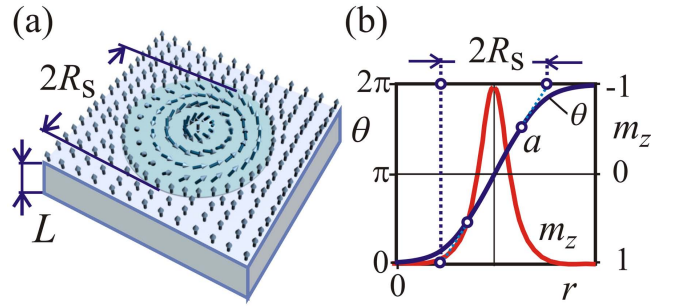


FIG. 1: (a) Axisymmetric isolated skyrmion with the core diameter $2R_s$ in a thin magnetic layer of thickness L . (b) The magnetization profile along the diameter cross-section $\theta(r)$ and the perpendicular magnetization $m_z(r)$ indicate a strong localization of the skyrmion core; $a(r_0, \theta_0)$ is the inflection point and the core radius R_s is derived from Eq. (6).

applicable to a broad range of material parameters. This is the first step towards a detailed calculation of the properties and behavior of chiral isolated skyrmions in layer systems.

As a model we consider a thin layer of a uniaxial ferromagnet with intrinsic or induced Dzyaloshinskii-Moriya couplings. The micromagnetic energy density of the layer [1, 3]

$$w = A(\text{grad}\mathbf{M})^2 - \mathbf{M} \cdot \mathbf{H} - K(\mathbf{M} \cdot \mathbf{n})^2 + w_d + w_D \quad (1)$$

includes exchange energy with stiffness A , uniaxial anisotropy with constant K (\mathbf{n} is a unity vector perpendicular to the layer surface), Zeeman, stray-field (w_d) and DM (w_D) energies [3, 9]. The chiral DM couplings are written as antisymmetric differential forms

$$\Lambda_{ij}^{(k)} = M_i \frac{\partial M_j}{\partial x_k} - M_j \frac{\partial M_i}{\partial x_k}, \quad (2)$$

that are known as Lifshitz invariants [1].

Introducing spherical coordinates for the magnetization $\mathbf{M} = M(\sin \theta \cos \psi, \sin \theta \sin \psi, \cos \theta)$ and cylindrical coordinates for the spatial variable $\mathbf{r} = (r \cos \varphi, r \sin \varphi, z)$

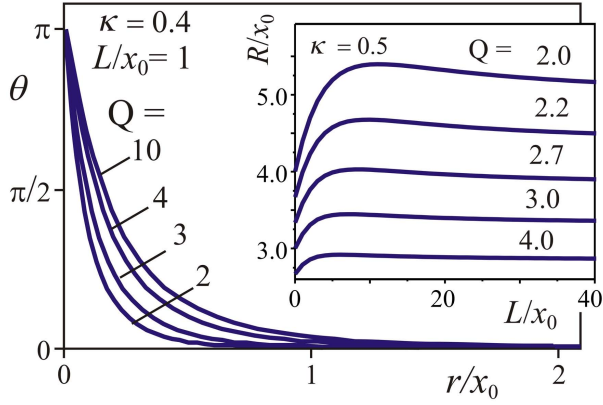


FIG. 2: Equilibrium magnetization profiles $\theta(r)$ for model (3) with $H = 0$, $\kappa = 0.4$, $L/x_0 = 1$ and different values of Q demonstrate a strong localization of the skyrmion core. Inset shows the reduced skyrmion core sizes R as a function of the reduced layer thickness L/x_0 derived by minimization of $\Phi(R)$ (Eq. (7)).

one can show that the equations minimizing functional (2) include axisymmetric localized solutions of the type $\theta(\rho)$, $\psi(\varphi)$ (Fig. 1). The solutions $\psi(\phi)$ depend on the magnetic symmetry [2]. In this paper we consider stray-field free configurations $\psi = \varphi + \pi/2$ arising in cubic helimagnets (crystal classes 23 (T) and 432 (O)) and in uniaxial ferromagnets with $n22$ (D_n) symmetry ($n = 3, 4, 6$) [2, 3]. For these handed ferromagnets the part of the Dzyaloshinskii-Moriya energy responsible for the stabilization of skyrmions (i.e. that with in-plane gradients) can be written as $\tilde{w}_D = D(\Lambda_{xz}^{(y)} - \Lambda_{yz}^{(x)})$ where the D is the Dzaloshinskii constant [2]. The total energy of the axisymmetric string in the layer of thickness L can be written in the following reduced form $W = 2\pi AL\tilde{w}$

$$\tilde{w} = \int_0^\infty \left[\left(\theta_\rho^2 + \frac{\sin^2 \theta}{\rho^2} \right) + \frac{4\kappa}{\pi} \left(\theta_\rho + \frac{\sin \theta \cos \theta}{\rho} \right) + \sin^2 \theta + (H/H_a)(1 - \cos \theta) + \tilde{w}_d(\rho, L)/Q \right] \rho d\rho. \quad (3)$$

Here, we use a new spatial variable $\rho = r/x_0$ and characteristic parameters

$$x_0 = \sqrt{\frac{A}{K}}, \quad H_a = \frac{K}{M}, \quad Q = \frac{K}{2\pi M^2}, \quad \kappa = \frac{\pi D}{4\sqrt{AK}}, \quad (4)$$

where x_0 is the Bloch wall thickness, H_a is the anisotropy field, Q is the quality factor [9], and the parameter κ describes the relative contribution of the DM energy. For $\kappa > 1$ chiral modulations in form of helices or skyrmion lattices become equilibrium states in bulk magnets [2]). The stray-field energy of the axisymmetric string \tilde{w}_d is derived by solving the corresponding magnetostatic problem [12]: $\tilde{w}_d(\rho, L) = (1 - 2\sin^2(\theta/2))\Omega(\rho, L)$

$$\Omega(\rho, L) = \frac{x_0}{L} \int_0^\infty (1 - \cos \theta)\Xi(\rho, \xi, x_0/L)\xi d\xi, \quad (5)$$

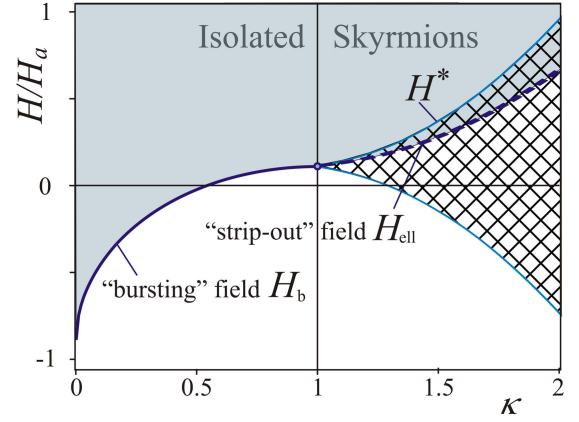


FIG. 3: The magnetic phase diagram in reduced variables κ and applied magnetic field H/H_a for fixed values of Q and the reduced layer thickness L/x_0 indicate the existence region of isolated skyrmions. In the double-hatched area spatially modulated phases (helicoids and skyrmion lattices) correspond to the equilibrium state of the film.

where $\Xi(\rho, \xi, x) = \int_0^\infty J_0(\xi\nu)J_0(\rho\nu)[1 - \exp(-\nu x)]d\nu$, $J_0(x)$ are the zero-order Bessel functions. The equations minimizing the functional W (3) with boundary conditions $\theta(0) = \pi$, $\theta(\infty) = 0$ yields the magnetization profiles for skyrmions $\theta(r)$ (Fig. 1) in the phase space of the four control parameters, κ , H/H_a , Q , L/x_0 .

Typical solutions $\theta(r)$ derived by numerical minimization of energy functional (3) are presented in Fig. 2. In a broad range of the control parameters the skyrmion profiles $\theta(r)$ consist of strongly localized arrow-like cores with linear variation of the angle $((\pi - \theta) \propto r)$ and exponential "tails" with $\theta \propto \kappa \exp(-r/x_0)$. A skyrmion core radius can be defined as

$$R_s = r_0 - \theta_0(d\theta/dr)_0^{-1}. \quad (6)$$

where (r_0, θ_0) are the coordinates of the inflection point a and $(d\theta/dr)_0$ is the derivative in this point (Fig. 1) [10].

The results in Fig. 2 demonstrate a variation of the skyrmion structure under the influence of magneto-dipole forces (parameters Q and L/x_0). This allows to adjust the skyrmion structure and size by the variation of the layer thickness L or the value of the quality factor Q .

In the phase diagram in reduced parameters κ , H/H_a and with fixed values of Q and L/x_0 (Fig. 3) we indicate the existence area of isolated skyrmions. Obviously skyrmions exist even in very high fields without collapse. At low fields the existence region of skyrmions is bound by several critical lines (Fig. 3). They remain stable in zero and negative field for $\kappa < 1$. At a certain critical "bursting" field H_b the skyrmion cores expand into a homogeneous state with magnetization parallel to the applied field. For $\kappa > 1$ skyrmions either condense into lattices on the transition line H^* or strip out into a helical

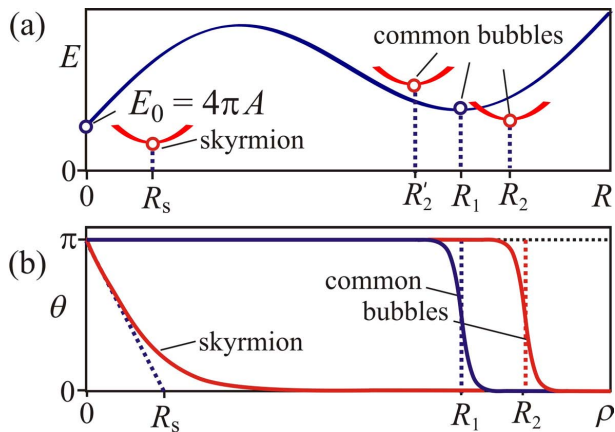


FIG. 4: Energy E of isolated bubbles and skyrmions as a function of their sizes (a) and the corresponding magnetization profiles $\theta(\rho)$ (b) for a centrosymmetric magnet ($D = 0$) and that with finite Dzyaloshinskii-Moriya energy ($D \neq 0$).

structure at a lower field H_{ell} . All these exceptional features of chiral skyrmions rely on the *topological and energetic* stabilization of their core structure by chiral DM couplings. Therefore, chiral skyrmions are fundamentally different from cylindrical *bubble* domains [9], which are intrinsically unstable and only arise by the surface depolarization and the tension of ordinary domain walls as an effect of the shape of a magnetized body.

In Fig. 4 we demonstrate how axisymmetric solutions for model (3) with $D = 0$ (thin (blue) lines) transform into solutions with DM interactions (thick (red) lines). For $D = 0$ only solutions for cylindrical domains (bubbles) exist as metastable states in a certain range of parameters H/H_a , Q , L/x_0 [12]. Usually bubble profiles $\theta(r)$ consist of an extended core with $\theta = \pi$ separated by a thin domain wall from the surrounding homogeneously magnetized area with $\theta = 0$ (Fig. 4 b) [9, 11, 12]. In Fig. 4 a energy (3) plotted as a function of the bubble core size $E(r)$ (blue line) indicates a metastable solution for $r = R_1$. Under the influence of DM interactions the profile of the energy density is modified and includes solutions for skyrmions with fixed rotation sense and finite radius $r = R_s$, and solutions for isolated bubbles, which may have different rotation sense of the magnetization ($r = R_2$ and $r = R_2'$) (red lines). The coexistence of skyrmion and bubble solutions occurs in a rather narrow range of the material parameters. Outside this area bubbles are unstable and only skyrmions can arise in the film.

In order to elucidate the physical mechanisms for the stabilization of chiral skyrmions in thin magnetic layers, a simplified semi-quantitative discussion is useful. The profiles $\theta(r)$ in the skyrmion center are linear. The strong localization of its core allows to use a linear ansatz $\theta = \pi(1 - r/R)$, ($0 < r < R$), $\theta = 0$, ($r > R$) as a suitable approximation for skyrmion solutions. With this trial

function the equilibrium sizes of the skyrmion are derived by minimization of the function

$$\Phi = \tilde{A}(H, Q)\nu^2 - 2\kappa(x_0/L)\nu + \nu^3 G(\nu)/Q, \quad \nu = R/L, \quad (7)$$

$G(\nu) = 2 \int_0^1 \cos(\pi\tau)\tau d\tau \int_0^1 \cos^2(\pi\xi/2) \Xi(\tau, \xi, \nu) \xi d\xi$ with function $\Xi(\tau, \xi, x)$ introduced in Eq. (5), $\tilde{A}(H, Q) = [1 + 8(1 - 4/\pi^2)(H/H_a) + (2/Q)(1 - 2/\pi^2)]$. The linear term proportional to κ is crucial for the existence of solutions with finite R . The "stiffness" coefficient \tilde{A} includes uniaxial anisotropy, stray-field and Zeeman energy contributions. Finally, the self dipole-dipole energy of the skyrmion $G(\nu)$ introduces a dependence of its size on the layer thickness L (Fig. 2 Inset).

Recent experiments in nanolayers of magnetic materials with intrinsic (cubic helimagnets $\text{Fe}_{0.5}\text{Co}_{0.5}\text{Si}$ and FeGe [7]) and with induced chirality (Fe/W bilayers) [8]) report observations of bound skyrmion states (lattices) (regions with $\kappa > 1$ in Fig. 3). Isolated skyrmions with $R_s \approx 45$ nm have been observed in a $\text{Fe}_{0.5}\text{Co}_{0.5}\text{Si}$ nanolayer ($L = 20$ nm) in the applied field larger than the critical field $H^* \approx 50$ mT (Fig. 3) [7]. By using experimental data from Refs. [7, 13] we found that for this sample $\kappa = 1.75$ and $x_0 = 16$ nm. Our model results corroborate the identification of the observed magnetization patterns as chiral skyrmions.

In conclusion, in magnetic layers with intrinsic or induced DM interactions isolated skyrmions with well-defined sized can exist as *regular* solutions of micromagnetic equations in a broad range of the material parameters (Figs. 2, 3). Chiral skyrmions as particle-like spots of reverse magnetization can be considered as the smallest conceivable micromagnetic configuration. Importantly and in contrast to alternative and traditional storage technologies based on highly coercive or patterned media, chiral skyrmions can exist in *magnetically soft* nanolayers even at zero field, when sufficiently strong DM interactions can be induced them. In such materials, chiral skyrmions can be easily induced, transported, and controlled, e.g., by electric currents and applied magnetic fields. Stable chiral skyrmions in extended layer systems are promising objects for novel types of magnetic data storages, but also for logical bit-wise operations in extended layer systems.

The authors thank G. Bihlmayer, S. Blügel, M. Bode, A.A. Leonov, and H. Wilhelm for helpful discussions.

* Electronic address: u.roessler@ifw-dresden.de

- [1] I. E. Dzyaloshinskii, Sov. Phys. JETP **19**, 960 (1964).
- [2] A.N. Bogdanov and D.A. Yablonsky, Zh. Eksp. Teor. Fiz. **95**, 178 (1989) [Sov. Phys. JETP **68**, 101 (1989)]; A. Bogdanov and A. Hubert, J. Magn. Magn. Mater. **138**, 255 (1994).

- [3] U.K. Rößler et al., Nature **442**, 797 (2006), U.K. Rößler et al., J. Phys.: Conf. Ser. In press (2011) (see also arXiv:1009.4849).
- [4] N.S. Kiselev et al., Phys. Rev. B **81**, 054409 (2010); Appl. Phys. Lett., **91**, 132507 (2007); **93**, 162502 (2008); C. Bran et al., Phys. Rev. B **79**, 024430 (2009).
- [5] M. Schneider et al., Appl. Phys. Lett., **77**, 2909 (2000); A. Wachowiak et al., Science **298**, 577 (2002); A. B. Butenko et al., Phys. Rev. B **80**, 134410 (2009).
- [6] A. N. Bogdanov, U. K. Rößler, Phys. Rev. Lett. **87**, 037203 (2001).
- [7] X. Z. Yu et al., Nature, **465**, 901 (2010); Nature Mat. **10**, 106 (2011).
- [8] S. Heinze et al., submitted to Nature Physics (2011) (see also APS March Meeting 2010, March 15-19,2010, abstract L34.014).
- [9] A. Hubert, R. Schäfer, *Magnetic Domains* (Springer, Berlin, 1998).
- [10] A. Bogdanov and A. Hubert, J. Magn. Magn. Mater. **195**, 182 (1999); phys. stat. sol. (b) **186**, 527 (1994).
- [11] A. A. Thiele, J. Appl. Phys. **41**, 1139 (1970); Bell System Tech. Journal **48**,3287 (1969).
- [12] Y. Tu, J. Appl. Phys. **42**,5704 (1971); W. J. DeBonte, J. Appl. Phys. **44**,1793 (1973).
- [13] J. Beille et al., J. Phys. F, **11**, 2153 (1981).